

GS-Phong: Meta-Learned 3D Gaussians for Relightable Novel View Synthesis

Yumeng He Yunbo Wang* Xiaokang Yang
MoE Key Lab of Artificial Intelligence, AI Institute,
Shanghai Jiao Tong University
{ymhe, yunbow, xkyang}@sjtu.edu.cn

June 3, 2024

Abstract

Decoupling the illumination in 3D scenes is crucial for novel view synthesis and relighting. In this paper, we propose a novel method for representing a scene illuminated by a point light using a set of relightable 3D Gaussian points. Inspired by the Blinn-Phong model, our approach decomposes the scene into ambient, diffuse, and specular components, enabling the synthesis of realistic lighting effects. To facilitate the decomposition of geometric information independent of lighting conditions, we introduce a novel bilevel optimization-based meta-learning framework. The fundamental idea is to view the rendering tasks under various lighting positions as a multi-task learning problem, which our meta-learning approach effectively addresses by *generalizing the learned Gaussian geometries not only across different viewpoints but also across diverse light positions*. Experimental results demonstrate the effectiveness of our approach in terms of training efficiency and rendering quality compared to existing methods for free-viewpoint relighting.

1 Introduction

Learning decoupled illumination components (ambient, diffuse, specular, etc.) from a small set of unstructured photographs is essential in 3D rendering, enabling the creation of lighting effects interacting with 3D objects. Recent advances in learning-based volume rendering, such as Neural Radiance Fields (NeRF) [13] and 3D Gaussian Splatting (3DGS) [7], have provided various solutions for the task of scene relighting [18, 34, 20, 37, 22, 19, 4, 28]. The NeRF-like implicit radiance representation facilitates the calculation of accumulated opacity along a ray, which enables the synthesis of realistic shadow effects within the scene. A typical method is to employ separate neural networks (*e.g.*, in NRHints [32]): one

*Corresponding author.

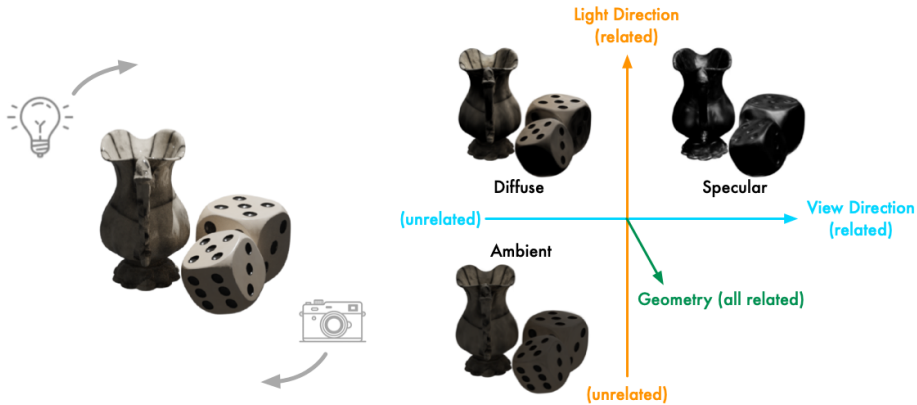


Figure 1: **Left:** Demonstration of the *One Light At a Time* (OLAT) training setup, which involves time-varying light conditions in conjunction with a monocular camera. **Right:** The decomposed illumination components by GS-Phong, which leverage specific physical priors related to light direction, view direction, and geometries.

for modeling the density field and one for modeling the light transport. However, this approach may potentially limit the model’s ability to generalize to more complex, out-of-distribution lighting conditions. Moreover, these approaches require substantial training time, often exceeding half a day.

The emergence of 3D Gaussian Splatting has revolutionized 3D reconstruction modeling by significantly reducing both training and inference time. Nevertheless, the explicit representation of Gaussian points brings difficulty for the computation of shadows, a vital component in disentangling scene characteristics from lighting effects. Recent studies have explored learning the bidirectional reflectance distribution function (BRDF) from *multi-view* images captured under consistent lighting conditions [26, 9, 6, 11, 3, 2]. With the learned sophisticated BRDF properties, these methods can handle the relighting tasks given novel environmental maps that represent the light and the surroundings of a 3D scene. However, these approaches require a substantial volume of images captured under individual lighting conditions, and are unsuitable for the One Light At a Time (OLAT) setting, where the scene is lit by a moving point light and the training data is captured by a monocular camera, as shown in Figure 1.

A deeper understanding of object geometries and materials is important for the simulation under various lighting conditions, as the direction in which light is reflected depends on the type of material and the normal direction of an object’s surface. However, in the OLAT setup, existing 3DGS-based methods struggle to obtain consistent inference of the geometries of the objects. This challenge arises because the perceived color at the same 3D location may change rapidly as the lighting condition changes. In brief, we try to learn a rendering function $C \sim F(V, L; \hat{G})$ in OLAT, where C is the output color and \hat{G} is the optimized geometric parameters. When the view direction V and the light position L

change at the same time, it increases the ambiguities of \hat{G} and consequently increases the challenges of disentangling the true light effects.

To alleviate the learning difficulty, we propose a simple yet effective illumination decoupling model named GS-Phong, which has two main technical contributions. First, our approach integrates different physically inspired priors into the learning process of individual illumination components, motivated by the Blinn-Phong model [1]. The fundamental idea is to decouple the ambient, diffuse, and specular light transport, as well as the shadows according to their different dependencies on V , L , and \hat{G} (Figure 1). For example, the intensity of the diffuse color varies with the normal direction of the Gaussian point along with the light directions, while the specular is dependent on all components in (V, L, \hat{G}) . The second contribution of our approach is to innovatively frame OLAT as a multi-task learning problem, viewing the rendering task under specific lighting positions as a separate task. Accordingly, we present a meta-learning algorithm to learn uniform Gaussian geometries that are more generalizable across a wide diversity of view directions or light directions. Specifically, in the inner optimization loop, we update the model from the last iteration for each task separately; while in the outer optimization loop, we perform a global update utilizing the derived model from the inner loop across all tasks, where the model parameters (both Gaussian attributes and shadow coefficients) are collectively updated. We evaluate GS-Phong on both synthetic and real-world OLAT datasets for novel view synthesis and relighting, and demonstrate its superior performance compared with existing 3DGS-based approaches. Besides, we provide further results to validate the respective effectiveness of the proposed methods, including the decomposed rendering pipeline based on the Phong model and the geometry optimization method based on meta-learning.

In summary, our work brings the following contributions:

- We propose GS-Phong, a novel modification of 3DGS that incorporates physical priors from the Phong model to decouple different illumination components in 3D rendering. GS-Phong enables realistic novel view synthesis with unseen lighting conditions.
- We introduce a meta-learning procedure for GS-Phong, which is novel in volume rendering. The key idea is to use bilevel optimization to derive uniform geometric knowledge that *generalizes not only across different viewpoints but also across diverse light positions*.

2 Problem Definition of OLAT

“One Light At A Time” (OLAT) refers to a specialized setting in the realm of 3D reconstruction (Figure 1). This involves illuminating the subject with a single point light in sequential exposures, capturing one image at each light position. Each capture makes up a tuple $\{\mathcal{I}, \mathcal{V}, \mathcal{L}\}$, where \mathcal{V} is the camera parameter and \mathcal{L} contains lighting information. In point-light scenes, \mathcal{L} includes the position and intensity of the light. For the specific setups in our work, GS-Phong is trained

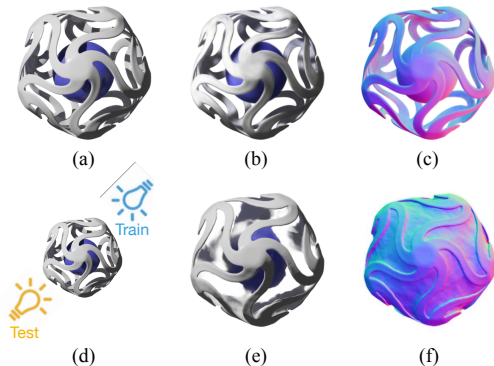


Figure 2: The results of existing 3DGS-based and NeRF-based relighting techniques (*i.e.* NRHints [32]) evaluated on out-of-distribution light positions. (a) ground truth image, (b)-(c) NVS rendering and normal prediction by GS-Phong, (d) OOD experiment setting, (e)-(f) NVS rendering and normal prediction by Zeng et al. [32].

under a set of randomly captured images $\{I\}_N$. Each image is grouped with its camera parameter and lighting information including light position and colors (light intensity is not included). Notably, unlike the “multiple lights, multiple cameras” setup¹ that necessitates multiple time-aligned cameras, OLAT requires only one monocular camera, which provides a much more convenient approach for data collection under the commonly observed light-changing scenarios in the real world.

Despite the data acquisition efficiency in OLAT, it poses a challenge to 3D reconstruction. With rapidly changing light positions in the training set, the color of a 3D point may change dramatically, potentially increasing ambiguities for the model in estimating its true color and geometry. In this work, we address this challenge using two techniques: First, we introduce strong physical priors through a differentiable Phong reflection model, aimed at decoupling the mixed components of light transport. Second, as an early attempt in volume rendering, we perform bilevel optimization-based meta-learning to facilitate the estimation of light-independent geometric information.

3 Preliminaries

3.1 3D Gaussian Splatting

Our method builds upon 3D Gaussian Splatting (3D-GS) [7], which employs explicit Gaussian points for 3D scene representation. Each Gaussian’s geometry is characterized by an opacity $o \in [0, 1]$, a center point $\mu \in \mathbb{R}^{3 \times 1}$ and a covariance

¹In the “multiple lights, multiple cameras” training set, for each lighting condition, multiple images are taken simultaneously to capture various perspectives of the scene.

matrix $\Sigma \in \mathbb{R}^{3 \times 3}$:

$$G(\mathbf{X}) = e^{-\frac{1}{2}(\mathbf{X}-\mu)^T \Sigma^{-1}(\mathbf{X}-\mu)} \quad (1)$$

where the covariance matrix Σ can be decomposed into a scaling matrix $S \in \mathbb{R}^{3 \times 1}$ and a quaternion-parameterized rotation matrix $R \in \mathbb{R}^{3 \times 3}$ to enable differentiable optimization:

$$\Sigma = R S S^T R^T \quad (2)$$

To render an image from a given viewpoint, 3D-GS utilize splatting technique to cast Gaussians within the view frustum onto the camera plane. The projected 2D covariance matrix Σ' in camera coordinates can be computed as $\Sigma' = J W \Sigma W^T J^T$, where W and J denote the viewing transformation and the Jacobian of the affine approximation of the projective transformation, respectively. The color of each pixel \mathbf{p} is calculated by alpha-blending N ordered Gaussians $\{G_i | i = 1, \dots, N\}$ overlapping \mathbf{p} as:

$$\mathcal{C} = \sum_{i \in N} T_i \alpha_i \mathbf{c}_i \text{ with } T_i = \prod_{j=1}^{i-1} (1 - \alpha_j) \quad (3)$$

where α_i denotes the alpha value calculated by multiplying the opacity o with the 2D Gaussian contribution value derived from Σ' , and T_i denotes the accumulated transmittance along the ray.

Specifically, each Gaussian’s color is defined by spherical harmonics (SH) coefficients $\mathcal{C} \in \mathbb{R}^k$ (where k represents the degrees of freedom). While high-order SH coefficients can contribute to the overall lighting of a scene under various view directions, they are not specifically designed to handle view-dependent color directly, such as specular reflections and shadows.

3.2 Blinn–Phong Illumination Model

The Phong model is widely adopted in computer graphics for simulating the interaction of light with object surfaces [15]. In this model, the reflected light transport on a surface has three components: ambient (L_a), diffuse (L_d), and specular reflections (L_s). The ambient reflection component represents the constant illumination present in the environment, simulating how light scatters and reflects off other surfaces to establish a baseline level of brightness. The diffuse reflection component, governed by Lambertian diffusion law, illustrates the scattering of light in multiple directions upon striking a rough surface, leading to a matte appearance. This component is calculated based on the angle between the light direction (\mathbf{l}) and the surface normal (\mathbf{n}), ensuring that surfaces facing the light source appear brighter. The specular term is computed based on the angle between the light direction vector and the bisector (\mathbf{h}) between the view direction (\mathbf{v}) and the light direction (\mathbf{l}). The Phong model also incorporates a shininess exponent that governs the spread of the specular highlight, allowing the model to represent the surface’s glossiness. We select the Blinn–Phong model [1] to provide the illumination decomposition priors to 3DGS due to its simplicity and computational efficiency.

3.3 Empirical Findings

In the context of this paper, we mainly explore relighting methods within the scope of 3DGS, due to its advantages in explicitly representing the geometric nature of the 3D scenes. We have two empirical findings in the preliminary experiments. First, we witness significant degeneration in the performance of existing 3DGS-based relighting techniques [6] under the challenging OLAT training setup (please refer to Sec. 5 for details). Second, we also evaluate NRHints [32], the prior art in the NeRF-based models. We observe that it underperforms in testing scenarios with out-of-distribution (OOD) lighting positions (Figure 2), a feature that we believe should be crucial for relighting methods.

Specifically, in Figure 2, the lighting in the training set is arranged on one side of the hemisphere, while the lighting in the test set is arranged on the opposite side (cameras are located on both sides). In such an OOD relighting setup, the baseline model fails to produce reasonable rendering results. The decreased performance is attributed to the implicit modeling of shadows and specular illuminations in the NeRF-based model. In other words, inputting the point light source position into the network design limits its ability to generalize to more complex, OOD lighting conditions. In contrast, we propose an explicit approach to model the lighting information, which naturally enables the reconstruction and relighting under unseen OOD scenarios.

4 Method

In this section, we provide the technical details of GS-Phong. In Sec. 4.1, we propose a differentiable Phong model, which extends 3D Gaussian Splatting (3DGS) to OLAT settings. In Sec. 4.2, we introduce a meta-learning framework to train the proposed GS-Phong, treating OLAT as a multi-task learning problem. The main focus of this method is to produce more generalized geometric information across diverse lighting conditions. In Sec. 4.3, we discuss the complete three-stage training scheme of GS-Phong and the regularization terms applied to the learned geometries. We present an overview of our approach in Figure 3.

4.1 A Learnable Phong Model

The intuition of GS-Phong is to disentangle the illumination components by interacting learnable Gaussian points with rays from both the viewer and the light source, which borrows strong physical priors from the Phong model. The Phong model is an extreme simplification of how light behaves on the object’s surface, however, it is very efficient to compute. As discussed above, the Phong model simulates the ambient, diffuse, and specular lighting effects given a point light. It can be described as a function $f : \mathbb{R}^3 \rightarrow \mathbb{R}$ that takes a 3D point $\mathbf{x} : (x, y, z)$ as input and returns a real number which is the associated light intensity.

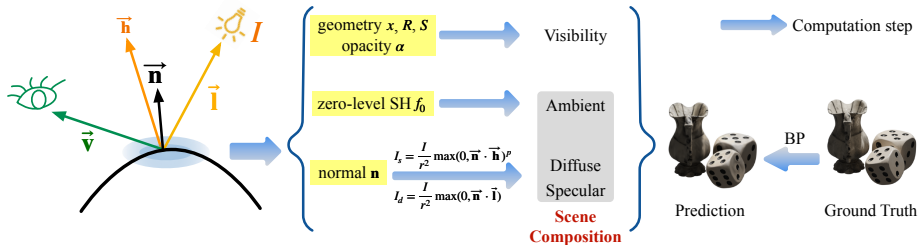


Figure 3: The model design of GS-Phong. The fundamental idea is to produce decomposed illumination results by interacting the learned Gaussian points with rays from both the viewer and the light source. We highlight the learned components in the computing pipeline of GS-Phong.

In GS-Phong, we extend the original 3DGS method by introducing the decoupled computation for different illumination components from the Phong model. Specifically, in addition to the basic attributes in 3DGS, including position \mathbf{x} , rotation R , scale S , opacity α , and Spherical Harmonic (SH) coefficients f , each Gaussian point is further associated with a normal vector \mathbf{n} , a 3-channel diffuse color k_d , and a 1-channel specular coefficient k_s . The newly added attributes endow the model with a better understanding of the lighting effects, thereby facilitating the learning process of light-independent object geometries. The overall color of a Gaussian point is formed as:

$$L_p = L_a + L_d + L_s = k_a I_a + \sum_{m \in \text{lights}} (k_d I_d + k_s I_s), \quad (4)$$

where $k_{\{a,d,s\}}$ and $I_{\{a,d,s\}}$ refer to the colors and intensities of each component.

For each training view, we successively model the ambient, diffuse, and specular colors of each Gaussian point. The ambient color adds constant color to account for disregarded illumination and fills in black shadows. In graphics and lighting applications, zero-order spherical harmonics (SH) coefficients typically represent the basic, uniform component of a function defined over the sphere, essentially the average or constant part of a lighting environment. Therefore, we restrict Gaussians' SH coefficients f to zero order, accounting for the ambient color in our setting.

We compute the diffuse and specular light transports by multiplying the color and intensity of each component. Derived from the Phong model, I_d and I_s are defined as:

$$I_d = \frac{I}{r^2} \max(0, \mathbf{n} \cdot \mathbf{l}), \quad I_s = \frac{I}{r^2} \max(0, \mathbf{n} \cdot \mathbf{h})^p, \quad (5)$$

where I is the light emitted intensity, \mathbf{l} is the point-to-light normalized vector, and $\mathbf{h} = \frac{\mathbf{v} + \mathbf{l}}{\|\mathbf{v} + \mathbf{l}\|}$ is the bisector of the point-to-camera normalized vector \mathbf{v} and \mathbf{l} . We model the coefficients k_d and k_s implicitly, where k_s is multiplied by the RGB color of the point light.

4.2 A Meta-Learning Framework of Light-Independent Geometries

The most challenging problem in OLAT is learning light-independent geometries. The appearance of identical points fluctuates significantly across different frames. Despite the effectiveness of GS-Phong in disentangling different illumination coefficients, most of its lighting components, including shadows, diffuse color, and specular color, are heavily dependent on the predicted normal vectors of the Gaussian points.

This “egg and chicken” problem of intertwined optimization of the illumination coefficients and object geometries prevents the model from learning the correct scene properties, making it prone to local optima. To address this issue, we present an early attempt in volume rendering that employs bilevel optimization-based meta-learning to enhance the estimation of light-independent geometric information. As illustrated in Alg. 1, we integrate information from multiple lighting conditions within a multi-task learning framework and update the model using second-order derivatives. The key idea is to encourage the learned geometries to generalize across different light positions.

Shadow computation. We calculate the shadow effects using a BVH-based ray tracing methodology. For each point, we determine light visibility by tracing a ray from the Gaussian’s mean location to the light source, then computing the cumulative transmittance of the ray as $T_i^{\text{light}} = \prod_{j=1}^{i-1} (1 - \alpha_j)$. Considering that only the diffuse and specular colors are influenced by incident light intensity, we update the color for each point by incorporating the light visibility factor into the diffuse and specular terms:

$$L_p = k_a I_a + T_i^{\text{light}} \times \sum_{m \in \text{lights}} (k_d I_d + k_s I_s). \quad (6)$$

However, directly integrating this module into the pipeline of GS-Phong is challenging. Due to the aforementioned “egg and chicken” problem, the model struggles to separate shadows from the scene, leading to inaccurate color predictions. Consequently, achieving accurate scene properties aligns with mastering shadow calculations.

Inner loop. To tackle the intertwined shadow learning problem inherent in OLAT, we integrate a meta-learning scheme into our training pipeline. In our meta-learning approach, the training set is partitioned into a support set and a query set according to different lighting conditions. Initially, all tasks start with the same model parameters, denoted as θ . Within each of the n iterations, the algorithm starts with the inner optimization loop. During this phase, each task selects a subset from the support set to update the model, resulting in θ^* . It first finetunes the Phong-related learnable parameters based on gradients derived from the shadow-free Phong model (Eq. (4)). Subsequently, the shadow coefficient is updated using losses obtained from the shadow-on Phong model (Eq. (6)), leveraging the updated Gaussian attributes. These per-task parameters are then utilized in the outer loop.

Algorithm 1 Meta-Training of GS-Phong.

- 1: **Input:** Training set $\{\mathcal{D}\}_i = \{\text{light pose, camera parameters, RGB image}\}_i$
 - 2: **Hyperparameters:** Learning rates $\alpha_1, \alpha_2, \beta$, training iterations n
 - 3: **Initialized parameters:** Shadow coefficient ϕ , pretrained Gaussian attributes $\{\theta\}_k = (x, S, \alpha, f, k_a, k_s)_k$,
 - 4: **for** n steps **do**
 - 5: Sample m support set $\mathcal{D}_i^{\text{sup}}$ and m query set $\mathcal{D}_i^{\text{query}}$ from $\{\mathcal{D}\}_i$ ▷ Using m tasks for one iteration
 - 6: **for** task i in $\{1 : m\}$ **do** ▷ Inner loop
 - 7: $\theta'_i \leftarrow \theta - \alpha_1 \nabla_{\theta} \mathcal{L}_{\text{phong}}(\theta, \mathcal{D}_i^{\text{sup}})$
 - 8: $\phi'_i \leftarrow \phi_i - \alpha_2 \nabla_{\phi} \mathcal{L}_{\text{shadow}}(\theta'_i, \phi, \mathcal{D}_i^{\text{sup}})$
 - 9: **end for**
 - 10: $\{\theta, \phi\} \leftarrow \{\theta, \phi\} - \beta \nabla_{\theta, \phi} \mathcal{L}_{\text{shadow}}(\theta'_i, \phi'_i, \mathcal{D}_i^{\text{query}})$ ▷ Outer loop
 - 11: **end for**
-

Outer loop. In the outer loop, a global update is performed across all tasks, where the model parameters (both Gaussian attributes and shadow coefficients) are collectively updated. During this phase, another subset from the query set is chosen to evaluate the updated model θ^* , yielding losses l_{θ^*} . These losses from all tasks are aggregated to formally update the model, and second-order gradients are backpropagated to θ through θ^* . Each task comes with its unique loss function. During training, the model continually shifts between these tasks. This structured approach, iterating through task-specific adaptation followed by a global update, enables the model to effectively learn generalizable features across diverse lighting conditions.

4.3 Optimization

We adopt a three-stage training scheme for effective learning. The first stage mirrors 3DGS, focusing solely on training the fundamental Gaussian attributes. This phase serves as a solid initialization for the model. In the second stage, we introduce normal tuning, recognizing that accurate Phong learning hinges greatly on precise normal vectors. Here, we incorporate the normal attribute into our training process. We supervise the predicted normal $\hat{\mathbf{n}}$ using depth-inferred pseudo-normal \mathbf{n} . Lastly, in the third stage, we integrate the diffuse, specular, and shadow coefficients, training all learnable parameters concurrently through our bilevel meta-learning framework.

Reconstruction loss. We follow 3DGS [7] to calculate the deviation of the predicted image from ground truth, which is L1 combined with a D-SSIM term:

$$\mathcal{L}_{\text{RGB}} = (1 - \lambda)\mathcal{L}_1 + \lambda\mathcal{L}_{\text{D-SSIM}}. \quad (7)$$

Normal-related loss. We initially implement regularization terms on the predicted normal to provide accurate information to Phong. For normal estimation, we follow GaussianShader [6] to compute the normal using Gaussian’s shortest

axis direction \mathbf{v} as well as two separate normal residuals, for outward or inward the normal:

$$\mathbf{n} = \begin{cases} \mathbf{v} + \Delta\mathbf{n}_1 & \text{if } \omega_{\mathbf{o}} \cdot \mathbf{v} > 0 \\ -(\mathbf{v} + \Delta\mathbf{n}_2) & \text{otherwise} \end{cases} \quad (8)$$

We compute the L1 loss of the predicted normal and depth-inferred normal: $\mathcal{L}_{\text{normal_pred}} = \|\bar{\mathbf{n}} - \hat{\mathbf{n}}\|^2$. We also use a residual regularization loss to prevent the normal residual from deviating too much from the shortest axis: $\mathcal{L}_{\text{normal_res}} = \|\Delta\mathbf{n}\|^2$. Furthermore, to ensure that the shortest axis of the Gaussian could represent the normal direction and to facilitate normal training, we constrain the minimum scale in Gaussian to be close to zero, effectively flattening the Gaussians towards a planar shape: $\mathcal{L}_s = \|\min(s_1, s_2, s_3)\|_1$. Finally, we have $\mathcal{L}_{\text{normal}} = \lambda_{\text{npred}}\mathcal{L}_{\text{normal_pred}} + \lambda_{\text{nres}}\mathcal{L}_{\text{normal_res}} + \lambda_s\mathcal{L}_s$.

Sparse loss. Like in GaussianShader, we use the sparse loss to encourage Gaussian spheres’ opacity values α to approach either 0 or 1:

$$\mathcal{L}_{\text{opacity}} = \frac{1}{|\alpha|} \sum_i [\log(\alpha_i) + \log(1 - \alpha_i)]. \quad (9)$$

We also add this loss on the light visibility term T_i^{light} to facilitate learning with opaque objects, thus we have: $\mathcal{L}_{\text{sparse}} = \lambda_{\text{opacity}}\mathcal{L}_{\text{opacity}} + \lambda_{\text{vis}}\mathcal{L}_{\text{vis}}$.

Smooth loss. To prevent high-frequency artifacts on the object’s surface, we follow the work from Qian et al. [16] to add a normal smooth loss using the rendered 2D normal map:

$$\mathcal{L}_{\text{smooth}} = \lambda_{\text{smooth}} \|\mathbf{n} - \text{sg}(g(\mathbf{n}, k))\|, \quad (10)$$

where $g(\cdot)$ is a Gaussian blur. The kernel size of the blurring k is set to 9×9 . We also add this loss to the rendered images of three separate components.

Diffuse prior loss. Given the physical insight that an object’s diffuse color is typically closely tied to its ambient color, often sharing the same color palette with one being a multiple of the other, naively learning the diffuse RGB coefficient may result in blurry outcomes. To address this, we devise a diffuse color regularization:

$$\mathcal{L}_{\text{diffuse}} = \lambda_{\text{diffuse}} \frac{1}{N} \sum_{i=1}^N \|\mathcal{I}_i^a - \mathbf{s} \cdot \mathcal{I}_i^d\|^2, \quad (11)$$

where N is the total number of points, \mathcal{I}_i^a and \mathcal{I}_i^d are three-channel vectors representing the i -th points’ RGB color. The idea is to restrict the diffuse RGB to be close to the multiple of the ambient color. The scaling factor \mathbf{s} is a three-channel vector, and can be obtained analytically by minimizing the loss function for each color channel:

$$\mathbf{s}_k = \frac{\sum_{i=1}^N \text{sg}(\mathcal{I}_{i,k}^a) \cdot \mathcal{I}_{i,k}^d}{\sum_{i=1}^N (\mathcal{I}_{i,k}^d)^2}, k \in \{0, 1, 2\}, \quad (12)$$

where $\text{sg}(\cdot)$ denotes the stop-gradient operation. This loss effectively restricts the diffuse RGB from becoming too chaotic and trapped in local minima.

During the three stages of our training, we gradually add in the above losses step by step:

$$\begin{aligned}
 \text{Stage 1 (Gaussian initialization): } & \mathcal{L}_{\text{stage1}} = \mathcal{L}_{\text{RGB}} + \mathcal{L}_{\text{sparse}} \\
 \text{Stage 2 (Normal finetuning): } & \mathcal{L}_{\text{stage2}} = \mathcal{L}_{\text{RGB}} + \mathcal{L}_{\text{sparse}} + \mathcal{L}_{\text{normal}} + \mathcal{L}_{\text{smooth}} \\
 \text{Stage 3 (Meta-learning): } & \mathcal{L}_{\text{stage3}} = \mathcal{L}_{\text{RGB}} + \mathcal{L}_{\text{sparse}} + \mathcal{L}_{\text{normal}} + \mathcal{L}_{\text{smooth}} + \mathcal{L}_{\text{diffuse}}
 \end{aligned}
 \tag{13}$$

4.4 Implementation Details

We implemented GS-Phong in PyTorch [14]. We use the Adam optimizer [8] with the same parameters as in Kerbl et al. [7]. We adopt the same set of hyper-parameters for all scenes in all of the three stages, which are detailed in Appendix A. Specifically, we use a standard exponential decay scheduling technique for the diffuse color prior to facilitate smooth training. We exponentially decay the diffuse color loss from 0.02 to 0.002 during the first $1k$ epochs in meta-learning stage, and fix it in the rest of the training. In our implementation, the first training stage lasts for $10k$ iterations, the second stage spans $5k$ iterations, and the third stage continues for $2k$ iterations. In total, the training process consumes approximately 40 minutes when executed on a single NVIDIA RTX3090 GPU.

5 Experiments

In this section, we present (i) qualitative and quantitative comparisons on both synthetic and real-world OLAT datasets with existing algorithms; (ii) GS-Phong’s capability of jointly estimating the scene’s geometry and inherent color by predicting lighting effects and removing shadows; (iii) Ablation studies of GS-Phong to investigate the effectiveness of each part of our methods.

5.1 Experimental Settings

We evaluate GS-Phong on three synthetic scenes and a real-world captured scene from Zeng et al. [32] with complicated object shapes and shadows to prove the ability of our model. For synthetic dataset, we select three scenes *Layered Woven Ball*, *Plastic Cup* and *Rubber Cup* representing different kinds of surfaces, where the Layered Woven Ball scene combines complex visibility and strong inter-reflections. We also test our method on a real captured scene *Cup Fabric*, which exhibits translucent materials (the cup), specular reflections of the balls, and an-isotropic reflections on the fabric. For each synthetic scene we use 500 OLAT images for training, and for real-world scene we only enlarge the training set size to 600.

We compare GS-Phong against both *3D Gaussian Splatting* [7] and two state-of-the-art 3D Gaussian illumination decomposition and relighting approaches,

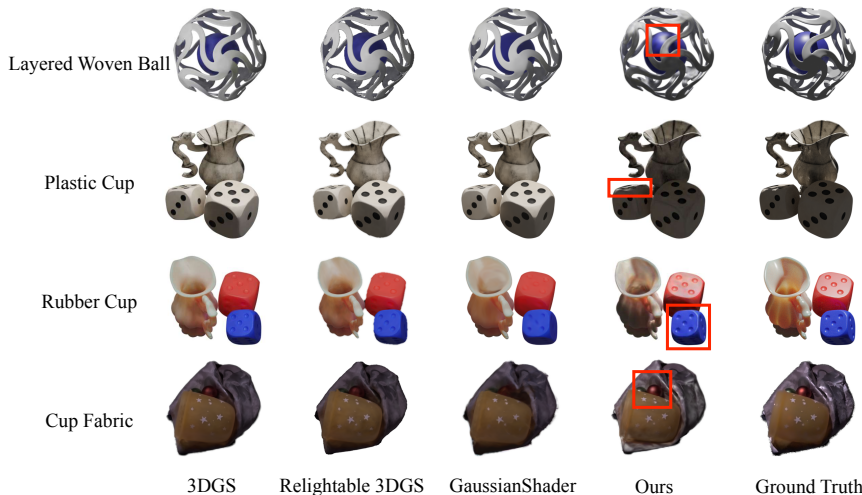


Figure 4: Quantitative results on three synthetic and one real-world *One Light At a Time (OLAT)* datasets. The highlighted areas demonstrate GS-Phong’s proficiency in accurately modeling specular and shadow regions, whereas baselines struggle to reconstruct these lighting effects.

including *Relightable 3D Gaussian* [5] and *GaussianShader* [6]. We train 3D Gaussian Splatting, GaussianShader and Relightable 3D-GS for 30k epochs, 30k epochs and 70k epochs respectively according to their original settings. The evaluation metrics to measure novel view rendering quality are reported in PSNR, SSIM [23], and LPIPS [35].

5.2 Comparison Results

Figure 4 and Table 1 present the quantitative and qualitative results of GS-Phong on free-viewpoint relighting tasks, where it outperforms all baseline methods by large margins. We present the best and second-best results in bold and underlined format, respectively. As shown in Figure 4, prior findings fail to

Table 1: Comparison of Methods on OLAT Datasets.

Method	Synthetic									Realworld		
	Layered Woven Ball			Plastic Cup			Rubber Cup			Cup Fabric		
	PSNR	SSIM	LIPIS	PSNR	SSIM	LIPIS	PSNR	SSIM	LIPIS	PSNR	SSIM	LIPIS
3D-GS [7]	19.55	0.9130	0.0580	21.13	0.9417	0.0470	23.22	0.9248	0.0796	24.58	0.9453	0.0835
Relightable 3D-GS [5]	19.62	0.9088	0.0610	21.07	0.9390	0.0502	23.20	0.9224	0.0838	24.55	0.9467	0.0792
GaussianShader [6]	19.62	0.9137	0.0586	20.92	0.9394	0.0500	23.12	0.9241	0.0833	23.12	0.9305	0.1081
Ours (w/o shadow)	<u>22.80</u>	<u>0.9446</u>	<u>0.0490</u>	<u>25.15</u>	<u>0.9553</u>	<u>0.0452</u>	<u>25.93</u>	<u>0.9375</u>	<u>0.0750</u>	<u>27.95</u>	<u>0.9577</u>	0.0834
Ours	29.51	0.9669	0.0388	30.04	0.9697	0.0385	28.73	0.9476	0.0691	28.42	0.9627	<u>0.0803</u>

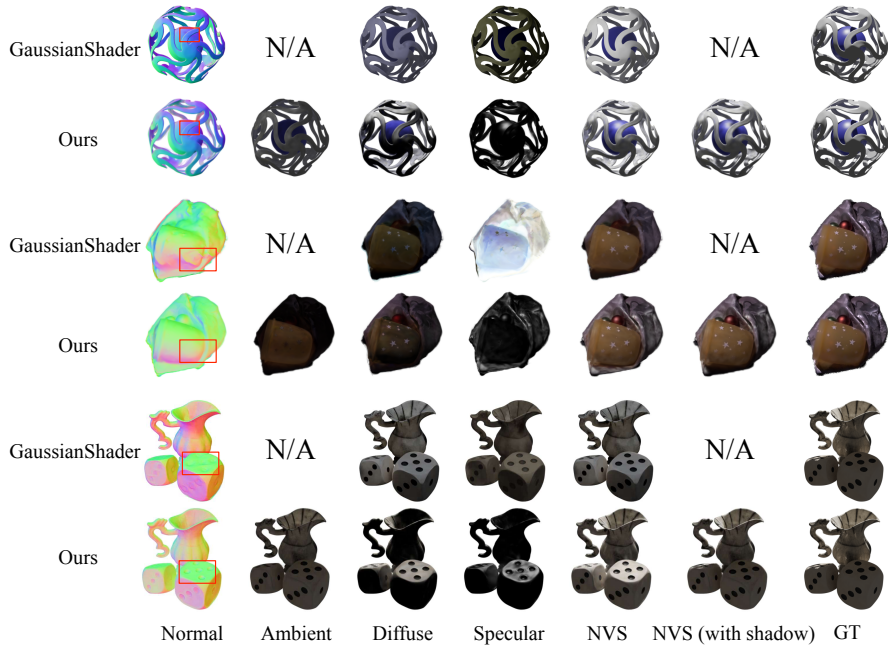


Figure 5: Quantitative comparison on illumination decoupling task with GaussianShader [6]. Key regions in the normal image are highlighted with red boxes. GS-Phong delivers effective decoupling results with accurate and smooth normals, whereas GaussianShader [6] fails to decompose the lighting effects and produces unrealistic normals marred by clear artifacts.

accurately extract shadows from the scene and severely conflate the lighting effect with the scene’s inherent color, resulting in an averaged color representation across different lighting conditions. They also fail to model correct shadow effects due to either inability to decouple OLAT scene [5, 6] or the absence of shadow computation module [6]. In contrast, GS-Phong effectively addresses these challenges by employing meta-learning and explicitly modeling the lighting information. This approach enables GS-Phong to correctly disentangle the various components of the scene, including accurate shadow representation and lighting effects. Additionally, we illustrate GS-Phong’s decomposition capability by comparing its decoupling results with GaussianShader [6]. As depicted in Figure 5, GS-Phong successfully decouples the scene into its correct components, whereas GaussianShader fails to accurately learn the lighting relationships, resulting in unrealistic outcomes. Overall, these results highlight the robustness and efficacy of GS-Phong in handling complex relighting tasks and achieving superior performance in scene decomposition.

Table 2: Ablation Studies on the Layered Woven Ball Scene.

	PSNR	SSIM	LPIPS
Full	29.51	0.9669	0.0388
w/o visibility sparse loss	28.38	0.9638	0.0401
w/o scene component smooth loss	25.83	0.9532	0.0457
w/o diffuse prior loss	26.07	0.9543	0.0452
w/o meta-learning (direct training)	19.65	0.8875	0.0754

5.3 Ablation Studies

We conduct a series of ablation studies to validate the effectiveness of meta-learning scheme and our geometry and color priors, using the Layered Woven Ball dataset from Zeng et al. [32]. The results are presented in Table 2.

Meta-learning As shown in Table 2 and discussed in Section 4.2, we employ a bilevel meta-learning training scheme to address the "chicken and egg" problem inherent in our learning task. our approach enables GS-Phong to converge correctly to the underlying geometry and color while simultaneously acquiring the illumination properties of the surfaces, paving a novel way for disentangling learning in reconstruction task. In the absence of this core component, our model struggles to converge smoothly and easily gets trapped in local minima. Specifically, without the meta-learning framework, the diffuse RGB color fails to converge correctly, resulting in a grey appearance.

Geometry priors We incorporate two geometry priors to the attributes of the Gaussian points. Firstly, We apply sparse regularization on the light visibility term T_i^{light} , encouraging the visibility values of Gaussians to approach either 0 or 1. This term indicates that a point is either fully illuminated or completely shadowed, facilitating learning with opaque objects. We also implement smooth regularizations on each component of the scene, calculated on the rendered images of ambient, diffuse, and specular color This prevents the model from producing unrealistic sharp color transitions. As shown in Table 2, these priors enhance the overall rendering performance by eliminating blurring and noisy estimations. More importantly, we observed gradient explosion phenomena when trained without the smooth prior, further illustrating its importance for robust training.

Color prior We adopt a simple way to model the diffuse reflectance RGB k_d as learnable parameters, providing flexibility in capturing complex surfaces. Nevertheless, this explicit representation lacks global coherence and may result in unrealistic, overly colorful outputs. Given the relative stability of ambient color during training, we enforce a constraint that ties the diffuse RGB closely to a multiple of the ambient color. This constraint prevents the diffuse RGB from becoming excessively chaotic and helps the model converge smoothly to

the correct color. Similar to the geometry priors, we observed gradient explosion issues when the diffuse prior was omitted, further underscoring its significance for stable training.

6 Related Work

6.1 Learning-based Volume Rendering

Volume rendering is a visualization technique that transforms 3D datasets into 2D images and is widely used in fields such as medical imaging, scientific visualization, and computational fluid dynamics. With recent advancements in deep learning technologies, learning-based methods have begun to be integrated into the field of volume rendering, including Neural Radiance Fields (NeRF) [13], neural Signed Distance Fields (SDF) [30], and 3D Gaussian Splatting [7]. These approaches not only enhance the visualization quality but also improve computational efficiency.

Introduced by Mildenhall et al. [13], Neural Radiance Fields (NeRF) represent a groundbreaking approach in the rendering of complex scenes with a high level of detail. NeRF employs a fully connected deep neural network to model volumetric scene function, encoding both color and density at any point in space using positional encoding and viewing directions. This model learns to render novel view synthesis by optimizing a photorealistic loss function, effectively enabling high-quality image synthesis from sparse viewpoints. This technique has spurred further research in neural rendering, which aims to efficiently interpolate and extrapolate complex 3D scenes [10, 33].

Signed Distance Fields (SDF) provide a geometric representation where each point in a volume corresponds to the shortest distance to a surface boundary, with the sign indicating whether the point is inside or outside the surface. While traditionally used in computer graphics for rendering and shape manipulation, recent advances have integrated SDF with deep learning to enhance both shape reconstruction and rendering quality, such as modeling the density using a certain transformation of a learnable SDF [30, 31], enabling robust handling of detailed and topologically complex structures.

Despite the high-quality synthesis ability of NeRF-like [10, 33] and SDF-like [30, 31] methods, these approaches require substantial training time, often exceeding half a day. The emergence of learnable 3D Gaussian Splatting [7] has revolutionized 3D reconstruction modeling by significantly reducing both training and inference time. 3D Gaussian Splatting is a technique used to convert point cloud data into a continuous volumetric representation, facilitating rendering and further processing. By applying a Gaussian kernel to each data point, this method smoothly interpolates the attributes across the volume. While not inherently a learning-based method, recent implementations [7] have incorporated machine learning to optimize kernel parameters dynamically, adapting to specific data characteristics or desired output quality. Such adaptive splatting techniques are increasingly used to enhance the efficiency of 3D and 4D reconstruction [26, 6, 12, 24, 29], demonstrating significant potential to handle diverse data types

and visualization requirements within short time. Among various learning-based volume rendering techniques, 3D Gaussian Splatting has gained particular attention for its practical efficiency and advanced reconstruction quality.

6.2 3D Relighting

3D Relighting refers to the process of dynamically altering the illumination of a 3D scene while preserving its geometry. By simulating the interaction between light and surfaces within the scene, this technique allows for the virtual manipulation of lighting conditions, including changes in intensity, direction, color, and distribution of light sources, to achieve desired visual effects. Recent advances in learning-based volume rendering have provided various solutions for this task, including methods based on NeRF [36, 21, 25, 19, 17, 18, 20, 19, 28], 3D Gaussian Splatting [26, 6, 5, 34], occupancy field [20] and so on, while most of these methods largely rely on learning the bidirectional reflectance distribution function (BRDF) from *multi-view* images captured under consistent lighting conditions [26, 9, 6, 5]. With the learned sophisticated BRDF properties, these methods can handle the relighting tasks given novel environmental maps that represent the light and the surroundings of a 3D scene.

The task of 3D relighting requires decomposing materials and lighting of a scene from multiple images, which is challenging due to its high-dimensional nature. Except for a few studies that aim at illumination decomposition and relighting under *One Light At a Time (OLAT) settings* [27, 36] - which are often too time-consuming due to NeRF’s implicit nature and volume rendering process) - most approaches [6, 5, 26, 9, 32] require a substantial volume of multi-view images captured under individual lighting conditions, and are unsuitable for OLAT settings. For instance, methods such as Wu et al. [26], Liang et al. [9], Jiang et al. [6] integrate the shadow effect into the objects’ color, therefore are effective only when the overall visibility (light occlusion correlations) of the scene remains constant.

Relightable 3D Gaussian [5] introduces an innovative Gaussian-based visibility calculation algorithm, simulating ray-tracing effects and incorporating visibility data into the spherical harmonics parameters of each point. Despite its efficiency in calculating and storing visibility information for Gaussian points under a fixed lighting condition, it requires training with images captured under consistent lighting to gather sufficient scene information without disturbances from changing lighting conditions.

NRHints [32] proposes an highly effective neural reflection model suitable for OLAT settings. However, it incorporates the point light position as a 3D input to the network, limiting the model to scenarios with only one point light source. Moreover, this model fails to generalize to unseen lighting conditions, such as scenarios where the lighting configurations in the training set differ from those in the testing set (as shown in Figure 2). These limitations are due to the implicit modelling nature that potentially limit the model’s ability to generalize to more complex, out-of-distribution (OOD) lighting conditions.

In contrast, our method model the lighting information in an explicit approach,

enabling robust reconstruction and relighting under unseen OOD scenarios. This explicit approach ensures better generalization and performance in diverse lighting conditions, addressing the limitations of previous methods.

7 Conclusions and Limitations

In conclusion, our proposed method for decoupling illumination in 3D scenes, which utilizes relightable 3D Gaussian points inspired by the Blinn-Phong model, effectively decomposes scenes into ambient, diffuse, and specular components for realistic lighting synthesis. By employing a novel bilevel optimization-based meta-learning framework, we can separate geometric information from lighting conditions, treating rendering tasks under various lighting positions as a multi-task learning problem. Our approach successfully generalizes learned Gaussian geometries across different viewpoints and light positions, as demonstrated by superior rendering quality in experimental results compared to existing methods for free-viewpoint relighting.

However, it’s important to note a limitation: while our approach successfully generalizes learned Gaussian geometries and colors across different viewpoints and light positions, further research is needed to enhance its robustness in handling extreme lighting conditions or complex scene geometries. Future work will focus on extending the model’s capabilities to address more challenging lighting scenarios and complex geometrical configurations, thereby broadening its applicability and performance in diverse settings.

Broader Impacts

The ability to synthesize realistic lighting effects and relight scenes from novel viewpoints could enhance the quality of visual media, including movies, video games, and virtual reality experiences. This could lead to more immersive and engaging entertainment, thereby benefiting society by providing richer visual experiences. However, the ability to manipulate lighting and scenes convincingly could be exploited to create deceptive or misleading content, including deepfakes or falsified evidence in legal or political contexts. This misuse could contribute to the spread of misinformation and undermine trust in visual media.

Dataset License

Our dataset includes assets modified from licensed assets acquired from Adobe Stock. According to Adobe’s Terms of License, we have obtained the full Adobe Stock license for our dataset.

References

- [1] James F Blinn. Models of light reflection for computer synthesized pictures. In *Proceedings of the 4th annual conference on Computer graphics and interactive techniques*, pages 192–198, 1977.
- [2] Mark Boss, Raphael Braun, Varun Jampani, Jonathan T Barron, Ce Liu, and Hendrik Lensch. Nerd: Neural reflectance decomposition from image collections. In *Proceedings of the IEEE/CVF International Conference on Computer Vision*, pages 12684–12694, 2021.
- [3] Mark Boss, Varun Jampani, Raphael Braun, Ce Liu, Jonathan Barron, and Hendrik Lensch. Neural-pil: Neural pre-integrated lighting for reflectance decomposition. *Advances in Neural Information Processing Systems*, 34:10691–10704, 2021.
- [4] Yeonjin Chang, Yearim Kim, Seunghyeon Seo, Jung Yi, and Nojun Kwak. Fast sun-aligned outdoor scene relighting based on tensorf. In *Proceedings of the IEEE/CVF Winter Conference on Applications of Computer Vision (WACV)*, pages 3626–3636, January 2024.
- [5] Jian Gao, Chun Gu, Youtian Lin, Hao Zhu, Xun Cao, Li Zhang, and Yao Yao. Relightable 3d gaussian: Real-time point cloud relighting with brdf decomposition and ray tracing. *arXiv preprint arXiv:2311.16043*, 2023.
- [6] Yingwenqi Jiang, Jiadong Tu, Yuan Liu, Xifeng Gao, Xiaoxiao Long, Wenping Wang, and Yuexin Ma. Gaussianshader: 3d gaussian splatting with shading functions for reflective surfaces. *arXiv preprint arXiv:2311.17977*, 2023.
- [7] Bernhard Kerbl, Georgios Kopanas, Thomas Leimkühler, and George Drettakis. 3d gaussian splatting for real-time radiance field rendering. *ACM Transactions on Graphics*, 42(4):1–14, 2023.

- [8] Diederik P Kingma and Jimmy Ba. Adam: A method for stochastic optimization. *arXiv preprint arXiv:1412.6980*, 2014.
- [9] Ruofan Liang, Huiting Chen, Chunlin Li, Fan Chen, Selvakumar Panneer, and Nandita Vijaykumar. Envidr: Implicit differentiable renderer with neural environment lighting. In *Proceedings of the IEEE/CVF International Conference on Computer Vision*, pages 79–89, 2023.
- [10] Lingjie Liu, Jiatao Gu, Kyaw Zaw Lin, Tat-Seng Chua, and Christian Theobalt. Neural sparse voxel fields. *Advances in Neural Information Processing Systems*, 33:15651–15663, 2020.
- [11] Yuan Liu, Peng Wang, Cheng Lin, Xiaoxiao Long, Jiepeng Wang, Lingjie Liu, Taku Komura, and Wenping Wang. Nero: Neural geometry and brdf reconstruction of reflective objects from multiview images. *ACM Transactions on Graphics (TOG)*, 42(4):1–22, 2023.
- [12] Jonathon Luiten, Georgios Kopanas, Bastian Leibe, and Deva Ramanan. Dynamic 3d gaussians: Tracking by persistent dynamic view synthesis. *arXiv preprint arXiv:2308.09713*, 2023.
- [13] Ben Mildenhall, Pratul P Srinivasan, Matthew Tancik, Jonathan T Barron, Ravi Ramamoorthi, and Ren Ng. Nerf: Representing scenes as neural radiance fields for view synthesis. *Communications of the ACM*, 65(1):99–106, 2021.
- [14] Adam Paszke, Sam Gross, Francisco Massa, Adam Lerer, James Bradbury, Gregory Chanan, Trevor Killeen, Zeming Lin, Natalia Gimelshein, Luca Antiga, et al. Pytorch: An imperative style, high-performance deep learning library. *Advances in neural information processing systems*, 32, 2019.
- [15] Bui Tuong Phong. Illumination for computer generated pictures. *Commun. ACM*, 18(6):311–317, jun 1975. ISSN 0001-0782. doi: 10.1145/360825.360839. URL <https://doi.org/10.1145/360825.360839>.
- [16] Guocheng Qian, Jinjie Mai, Abdullah Hamdi, Jian Ren, Aliaksandr Siarohin, Bing Li, Hsin-Ying Lee, Ivan Skorokhodov, Peter Wonka, Sergey Tulyakov, et al. Magic123: One image to high-quality 3d object generation using both 2d and 3d diffusion priors. *arXiv preprint arXiv:2306.17843*, 2023.
- [17] Kripasindhu Sarkar, Marcel C Böhler, Gengyan Li, Daoye Wang, Delio Vicini, Jérémy Riviere, Yinda Zhang, Sergio Orts-Escolano, Paulo Gotardo, Thabo Beeler, et al. Litnerf: Intrinsic radiance decomposition for high-quality view synthesis and relighting of faces. In *SIGGRAPH Asia 2023 Conference Papers*, pages 1–11, 2023.
- [18] Pratul P. Srinivasan, Boyang Deng, Xiuming Zhang, Matthew Tancik, Ben Mildenhall, and Jonathan T. Barron. Nerv: Neural reflectance and visibility fields for relighting and view synthesis. In *Proceedings of the IEEE/CVF Conference on Computer Vision and Pattern Recognition (CVPR)*, pages 7495–7504, June 2021.
- [19] Jia-Mu Sun, Tong Wu, Yong-Liang Yang, Yu-Kun Lai, and Lin Gao. Sol-nerf: Sunlight modeling for outdoor scene decomposition and relighting. In *SIGGRAPH Asia 2023 Conference Papers*, pages 1–11, 2023.

- [20] Marco Toschi, Riccardo De Matteo, Riccardo Spezialetti, Daniele De Gregorio, Luigi Di Stefano, and Samuele Salti. Relight my nerf: A dataset for novel view synthesis and relighting of real world objects. In *Proceedings of the IEEE/CVF Conference on Computer Vision and Pattern Recognition (CVPR)*, pages 20762–20772, June 2023.
- [21] Marco Toschi, Riccardo De Matteo, Riccardo Spezialetti, Daniele De Gregorio, Luigi Di Stefano, and Samuele Salti. Relight my nerf: A dataset for novel view synthesis and relighting of real world objects. In *Proceedings of the IEEE/CVF Conference on Computer Vision and Pattern Recognition*, pages 20762–20772, 2023.
- [22] Dongqing Wang, Tong Zhang, and Sabine Süsstrunk. Nemto: Neural environment matting for novel view and relighting synthesis of transparent objects. In *Proceedings of the IEEE/CVF International Conference on Computer Vision (ICCV)*, pages 317–327, October 2023.
- [23] Zhou Wang, Alan C Bovik, Hamid R Sheikh, and Eero P Simoncelli. Image quality assessment: from error visibility to structural similarity. *IEEE transactions on image processing*, 13(4):600–612, 2004.
- [24] Guanjuan Wu, Taoran Yi, Jiemin Fang, Lingxi Xie, Xiaopeng Zhang, Wei Wei, Wenyu Liu, Qi Tian, and Xinggang Wang. 4d gaussian splatting for real-time dynamic scene rendering. *arXiv preprint arXiv:2310.08528*, 2023.
- [25] Tong Wu, Jia-Mu Sun, Yu-Kun Lai, and Lin Gao. De-nerf: Decoupled neural radiance fields for view-consistent appearance editing and high-frequency environmental relighting. In *ACM SIGGRAPH 2023 conference proceedings*, pages 1–11, 2023.
- [26] Tong Wu, Jia-Mu Sun, Yu-Kun Lai, Yuewen Ma, Leif Kobbelt, and Lin Gao. Deferredrgs: Decoupled and editable gaussian splatting with deferred shading. *arXiv preprint arXiv:2404.09412*, 2024.
- [27] Yingyan Xu, Gaspard Zoss, Prashanth Chandran, Markus Gross, Derek Bradley, and Paulo Gotardo. Renerf: Relightable neural radiance fields with nearfield lighting. In *Proceedings of the IEEE/CVF International Conference on Computer Vision*, pages 22581–22591, 2023.
- [28] Siqi Yang, Xuanning Cui, Yongjie Zhu, Jiajun Tang, Si Li, Zhaofei Yu, and Boxin Shi. Complementary intrinsics from neural radiance fields and cnns for outdoor scene relighting. In *Proceedings of the IEEE/CVF Conference on Computer Vision and Pattern Recognition (CVPR)*, pages 16600–16609, June 2023.
- [29] Ziyi Yang, Xinyu Gao, Wen Zhou, Shaohui Jiao, Yuqing Zhang, and Xiaogang Jin. Deformable 3d gaussians for high-fidelity monocular dynamic scene reconstruction. *arXiv preprint arXiv:2309.13101*, 2023.
- [30] Lior Yariv, Jiatao Gu, Yoni Kasten, and Yaron Lipman. Volume rendering of neural implicit surfaces. *Advances in Neural Information Processing Systems*, 34: 4805–4815, 2021.

- [31] Zehao Yu, Songyou Peng, Michael Niemeyer, Torsten Sattler, and Andreas Geiger. Monosdf: Exploring monocular geometric cues for neural implicit surface reconstruction. *Advances in neural information processing systems*, 35:25018–25032, 2022.
- [32] Chong Zeng, Guojun Chen, Yue Dong, Pieter Peers, Hongzhi Wu, and Xin Tong. Relighting neural radiance fields with shadow and highlight hints. In *ACM SIGGRAPH 2023 Conference Proceedings*, pages 1–11, 2023.
- [33] Kai Zhang, Gernot Riegler, Noah Snaveley, and Vladlen Koltun. Nerf++: Analyzing and improving neural radiance fields. *arXiv preprint arXiv:2010.07492*, 2020.
- [34] Kai Zhang, Fujun Luan, Qianqian Wang, Kavita Bala, and Noah Snaveley. Physg: Inverse rendering with spherical gaussians for physics-based material editing and relighting. In *Proceedings of the IEEE/CVF Conference on Computer Vision and Pattern Recognition (CVPR)*, pages 5453–5462, June 2021.
- [35] Richard Zhang, Phillip Isola, Alexei A Efros, Eli Shechtman, and Oliver Wang. The unreasonable effectiveness of deep features as a perceptual metric. In *Proceedings of the IEEE conference on computer vision and pattern recognition*, pages 586–595, 2018.
- [36] Xiuming Zhang, Pratul P Srinivasan, Boyang Deng, Paul Debevec, William T Freeman, and Jonathan T Barron. Nerfactor: Neural factorization of shape and reflectance under an unknown illumination. *ACM Transactions on Graphics (ToG)*, 40(6):1–18, 2021.
- [37] Ruichen Zheng, Peng Li, Haoqian Wang, and Tao Yu. Learning visibility field for detailed 3d human reconstruction and relighting. In *Proceedings of the IEEE/CVF Conference on Computer Vision and Pattern Recognition (CVPR)*, pages 216–226, June 2023.

A Hyperparameters

The hyperparameters of GS-Phong are shown in Table 3.

Table 3: Hyperparameters of GS-Phong.

Name	Notation	Value
meta-training inner learning rate	α_1, α_2	10^{-8}
model learning rate	β_1	the same decay as 3D-GS[7]
RGB D-SSIM loss scale	λ	0.2
normal prediction loss scale	λ_{npred}	0.1
normal residual regularization scale	λ_{nres}	0.001
normal flatten loss scale	λ_{s}	0.00001
opacity sparse loss scale	λ_{opacity}	0.001
visibility sparse loss scale	λ_{vis}	0.01
smooth loss scale	λ_{smooth}	0.1